AMSR-E/Aqua L2B Global Swath Surface Precipitation GSFC Profiling Algorithm, Version 3

USER GUIDE

How to Cite These Data

As a condition of using these data, you must include a citation:

Kummerow, C., R. Ferraro, and D. Randel. 2015. *AMSR-E/Aqua L2B Global Swath Surface Precipitation GSFC Profiling Algorithm, Version 3*. [Indicate subset used]. Boulder, Colorado USA. NASA National Snow and Ice Data Center Distributed Active Archive Center.

https://doi.org/10.5067/AMSR-E/AE_RAIN.003. [Date Accessed].

FOR QUESTIONS ABOUT THESE DATA, CONTACT NSIDC@NSIDC.ORG

FOR CURRENT INFORMATION, VISIT https://nsidc.org/data/AE_Rain

National Snow and Ice Data Center

TABLE OF CONTENTS

1 DATA DESCRIPTION

1.1 Parameters

- Total Surface Precipitation Rate (mm/hr)
- Convective Surface Precipitation Rate (mm/hr)
- Liquid Surface Precipitation Rate (mm/hr)
- Precipitation Rate (mm/hr)
- Cloud Liquid Water/Ice (kg/m^2)

1.2 File Information

1.2.1 Format

AMSR-E collects 243 data points per scan for the 6.9 GHz to 36.5 GHz channels and 392 data points for the 89.0 GHz channel. Data are in Hierarchical Data Format – Earth Observing System (HDF-EOS) format. Refer to tables 1 and 2 regarding data field details.

Table 1. Data Field Notations

Float64:	64-bit (8-byte) floating-point integer
Float32:	32-bit (4-byte) floating-point integer
Int8:	8-bit (1-byte) signed integer
Int16:	16-bit (2-byte) signed integer

Table 2. Data Fields

Data Fields	Data Type	Dimensions	Description	Scale	Fill Value/No Value
Time	Float64	approximately 2000 scans	Scan start time in International Atomic Time in seconds with 01 January 1993 00:00:00 as the zero base (TAI93).	n/a	n/a
Latitude	Float32	392 x approximately 2000 scans	Latitude (-89.24 to 89.24)	n/a	99
Longitude	Float32	392 x approximately 2000 scans	Longitude (-180.0 to 180.0)	n/a	999

Data Fields	Data Type	Dimensions	Description	Scale	Fill Value/No Value
surfaceType	Int8	392 x approximately 2000 scans	10: Ocean 11: Sea ice 12: Partial sea ice 20: Land 30: Coast 31: Inland water	n/a	-99
pixelStatus	Int8	392 x approximately 2000 scans	If there is retrieval at a given pixel, pixelStatus explains the reason. 0: Valid pixel 1: Boundary error in landmask 2: Boundary error in sea-ice check 3: Boundary error in sea surface temperature 4: Invalid time 5: Invalid latitude/longitude 6: Invalid brightness temperature 7: Invalid sea surface temperature 8: No retrieval due to sea-ice over water 9: No retrieval due to sea-ice over coast 10: Land/coast screens not able to be applied 11: Failure in ocean rain - no match with database profile TBs 12: Desert screen 13: Snow climatology screen	n/a	n/a

Data Fields	Data Type	Dimensions	Description	Scale	Fill Value/No Value
QualityFlag	Int8	392 x approximately 2000 scans	QualityFlag indicates a generalized quality of the retrieved pixel. 0: High quality (retrieval is good) 1: Medium quality (use with caution) 2: Low quality (recommended qualitative use only) **Ocean Algorithm:** High: Good retrieval (uses entries from TRMM *a priori* database) Medium: Retrieval used extended database and/or expanded search radius for *a priori* database (see oceanExtendedDbase and/or oceanSearchRadius) Low: Retrieval used search radius to find matches in *a priori* database (see oceansearchRadius) **Land/Coast Algorithm:** High: Good retrieval Medium: Ambiguous pixel (see landScreenFlag) Low: Missing or unable to retrieve pixels (see pixelStatus)	n/a	-99

Data Fields	Data Type	Dimensions	Description	Scale	Fill Value/No Value
landAmbiguousFlag	Int8	392 x approximately 2000 scans	Defines codes for uncertain/ambiguous retrievals over land 0: No information 13: Ambiguous T22V / 2 different scattering screens 14: Cannot discriminate precipitation from cold surface 63: Light precipitation 64: Cold surface 65: Grody light precipitation 66: Huffman ambiguous -22: Desert screen -42: Snow climatology screen	n/a	n/a
landScreenFlag	Int8	392 x approximately 2000 scans	0: No information -31: Land retrieval found ice likely -41: Land retrieval found large polarization difference due to ice or sand -51: Warm 85H and Low 22V, or clear ocean likely in coast retrieval -61: probable coastline in coast retrieval	n/a	n/a
oceanExtendedDbase	Int8	392 x approximately 2000 scans	Percent of the extended database entries (i.e., beyond the TRMM database) used in the retrieval (range 0-100). 0: only the TRMM database entries used 1-99: % of the entries from the extended database used 100: Only the extended datase entries used	n/a	n/a

Data Fields	Data Type	Dimensions	Description	Scale	Fill Value/No Value
oceanSearchRadius	Int8	392 x approximately 2000 scans	Expansion of the search radius of the *a priori*database beyond the initial SST and TPW search range. 0: Default search radius used 1: Search radius expanded by +/- 1 mm in TPW and +/- 1 degree in SST N: Search radius expanded by +/- N mm in TPW and +/- N degrees in SST	n/a	-99
chiSquared	Int8	392 x approximately 2000 scans	Error diagnostic for Optimal Estimation calculation of TPW and wind speed. Values greater than the number of channels (9 for TMI) should be considered suspect, with values greater than 18 of limited use. Rainfall is possible above these values. Values could range from 0 to 10000, but should be less than 100.	n/a	n/a
probabilityOfPrecip	Int8	392 x approximately 2000 scans	A diagnostic variable, in percent, defining the fraction of raining vs. non-raining database profiles that make up the final solution. Values range from 0 to 100 percent.	n/a	-99

Data Fields	Data Type	Dimensions	Description	Scale	Fill Value/No Value
sunGlintAngle	Int8	392 x approximately 2000 scans	sunGlintAngle is the angular separation between the Reflected Satellite View Vector and the Sun Vector. When sunGlintAngle is zero, the instrument views the center of the specular (mirror-like) sun reflection. See Kummerow 2014 for more information. Values range from 0 to 180 degrees.	n/a	n/a
freezingHeight	Int16	392 x approximately 2000 scans	The height, in meters, of the 0°C isotherm above the earth ellipsoid.	n/a	-9999
surfacePrecipitation	Float32	392 x approximately 2000 scans	The instantaneous total precipitation rate at the surface for each pixel. Check pixelStatus for a valid retrieval. Values are in mm/hr.	n/a	-9999.9
convectivePrecipitation	Float32	392 x approximately 2000 scans	The instantaneous convective precipitation rate at the surface for each pixel. Check pixelStatus for a valid retrieval. Values are in mm/hr.	n/a	-9999.9
surfaceRain	Float32	392 x approximately 2000 scans	The instantaneous rain rate (liquid portion of precipitation) at the surface for each pixel. Check pixelStatus for a valid retrieval. Values are in mm/hr.	n/a	-9999.9
cloudWaterPath	Float32	392 x approximately 2000 scans	Total cloud liquid water in the column. Values range from 0 to 3.0 kg/m^2.	n/a	-9999.9

Data Fields	Data Type	Dimensions	Description	Scale	Fill Value/No Value
rainWaterPath	Float32	392 x approximately 2000 scans	Total rain water in the column. Values range from 0 to 10.0 kg/m^2.	n/a	-9999.9
iceWaterPath	Float32	392 x approximately 2000 scans	Total cloud ice in the column. Values range from 0 to 10.0 kg/m^2.	n/a	-9999.9
ReySeaSurfaceTemperature	Float32	392 x approximately 2000 scans	Optimum Interpolation Sea Surface Temperatures constructed by combining observations from different platforms (satellites, ships, buoys) on a regular global grid.	n/a	-9999.9

Note: Beginning with the algorithm version B04, data dimensions changed from 486 pixels to 392 pixels due to the loss of the 89 GHz A-horn.

1.2.2 File Contents

Each half-orbit granule is approximately 18 MB.

1.2.3 Naming Convention

This section explains the file naming convention used for this product with an example. The date and time correspond to the first scan of the granule.

Example file name:

AMSR_E_L2_Rain_V12_20070101023_D.hdf

AMSR_E_L2_Rain_X##_yyyymmddhhmm_f.hdf

Refer to Table 3 for the valid values for the file name variables listed above.

Table 3. Valid Values for the File Name Variables

Variable	Description
X	Product Maturity Code
##	file version number
yyyy	four-digit year

Variable	Description
mm	two-digit month
dd	two-digit day
hh	hour, listed in UTC time, of first scan in the file
mm	minute, listed in UTC time, of first scan in the file
f	orbit direction flag (A = ascending, D = descending)

Table 4. Valid Values for the Product Maturity Code

Variable	Description
P	Preliminary - refers to non-standard, near-real-time data available from NSIDC. These data are only available for a limited time until the corresponding standard product is ingested at NSIDC.
B	Beta - indicates a developing algorithm with updates anticipated.
T	Transitional - period between beta and validated where the product is past the beta stage, but not quite ready for validation. This is where the algorithm matures and stabilizes.
V	Validated - products are upgraded to Validated once the algorithm is verified by the algorithm team and validated by the validation teams. Validated products have an associated validation stage.

Table 5 provides examples of file name extensions for related files that further describe or supplement data files.

Table 5. Related File Extensions and Descriptions

Extensions for Related Files	Description
.jpg	Browse data
.qa	Quality assurance information
.ph	Product history data
.xml	Metadata files

1.3 Spatial Information

1.3.1 Coverage

This data set offers coverage of all ice-free and snow-free land and ocean between 89°24' N and -89°24' S latitudes.

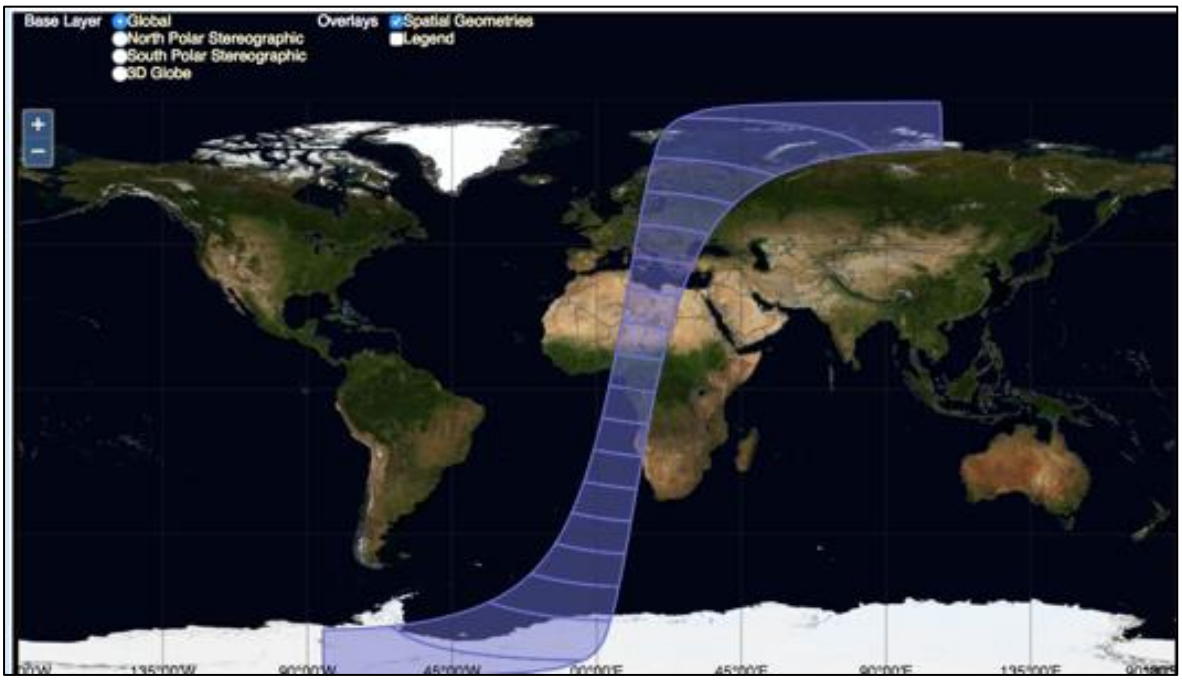

Figure 1. Spatial Coverage Map displaying one half orbit of the AMSR-E instrument. The map was created using Reverb | ECHO

1.3.2 Resolution

Data are 10 km resolution along the track and 5 km along scan.

1.4 Temporal Information

1.4.1 Coverage

Data were collected from 2002-6-1 to 2011-10-4.

1.4.2 Resolution

Each half-orbit swath spans approximately 50 minutes. The data sampling interval is 2.6 ms per sample for the 6.9 GHz to 36.5 GHz channels and 1.3 ms for the 89.0 GHz channel. A full scan takes approximately 1.5 seconds.

2 DATA ACQUISITION AND PROCESSING

2.1 Acquisition

The AMSR-E/Aqua L2B precipitation data (AE_Rain) are derived from AMSR-E/Aqua L2A Global Swath Spatially-Resampled Brightness Temperatures, Version 3.

2.2 Processing

2.2.1 Theory of Measurements

Satellite-based estimates of rain rate and rain type rely primarily on modeling the absorption and emission effects on microwave signals for specified cloud temperatures, water vapor, and hydro meteor profiles. Atmospheric transmittance windows below 20 GHz, from 30 GHz to 40 GHz, and at 90 GHz are used for rainfall monitoring. Below 20 GHz, rainfall absorption and emission are predominant, and ocean surfaces are warmer than the background radiation. Above 60 GHz, evidence of rainfall is primarily from scattering, where areas of heavy rainfall are colder than their backgrounds. Between 20-60 GHz, a combination of absorption and scattering is present.

A radiative transfer equation that includes absorption and scattering coefficients is the basis for deriving rain rate from brightness temperatures in this data set. The absorption and scattering coefficients, which are summarized in more detail in Kummerow and Ferraro 2006, are expressed as an integral over the range of rain drop sizes. Radiative transfer calculations are used to determine brightness temperatures given atmospheric temperature, water vapor, and hydrometeor profiles. These computations are carried out for the AMSR-E frequencies of 6.9, 10.7, 18.7, 36.6 and 89.0 GHz and 54-degree incidence angle, and for different freezing levels.

At all channels, brightness temperatures increase toward a maximum and then drop off as rainfall rates increase further. The main difference between channels is the range of rainfall rates for which the curve increases in the emission region and decreases in the scattering region (Kummerow and Ferraro 2006). The brightness temperature at low frequencies is primarily a function of absorption. The rain rate follows from the absorption coefficient implied by the measurements. Ice and snow are efficient scatterers of microwave radiation compared with rain. Since land background has a high emissivity, rainfall rate over land must be inferred from the ice-scattering signature, instead of relying on the emission signal from rain drops.

2.2.2 Derivation Techniques and Algorithms

This section covers the theoretical basis for the retrieval of liquid and solid precipitation from the AMSR-E radiometers. The algorithm is a Bayesian type algorithm, which searches an a priori database of potential rain profiles and retrieves a weighted average of these entries based upon an uncertainty weighted proximity of the observed Brightness Temperatures (Tb) to the simulated Brightness Temperatures corresponding to each rain profile. The a priori information is supplied by the TRMM radar/radiometer algorithm as detailed in Kummerow et al. (2010). The solution provides a mean rain rate as well as its uncertainty. The major sources of systematic errors in these algorithms are the quality of the a priori database, the estimate of the forward model uncertainty, and the ancillary information used to subset the a priori database.

2.2.2.1 Instantaneous Ocean Rainfall

The ocean algorithm uses a Bayesian approach in which the TRMM satellite is used to create an a priori database of observed cloud and precipitation profiles as described in Kummerow, et al. (2010). The profiles for the rain ocean procedure are grouped by SST and TPW. The individual pixels TPW and SST are used to retrieve a group of pixels from the database. If there are fewer than 1000 profile clusters found, the search radius is expanded. Once the database of representative profiles and Brightness Temperatures are generated, the algorithm uses a Bayesian inversion methodology in the following manner:

$$Pr(R|T_b) = Pr(R)*Pr(T_b|R)$$

Equation 1

Where:

Pr(R) = probability that a profile R will be observed

$Pr(T_b \mid R)$ = probability of observing the brightness temperature vector, T_b, given a specific rain profile R.

he first term on the right-hand side of Equation 1 is derived from the a priori database of rain profiles established by the radar/radiometer observing systems. The second term on the right-hand side is obtained from radiative transfer computations through the cloud model profiles. The formal solution to the above problem is presented in detail in Kummerow et al. (1996). In summary, the retrieval procedure composes a new hydrometeor profile by taking the weighted sum of structures in the cloud structure database that are radiometrically consistent with the observations. The weighting of each model profile in the compositing procedure is an exponential factor containing the mean square difference of the sensor observed brightness temperatures and a corresponding set of brightness temperatures obtained from radiative transfer calculations through the cloudy atmosphere represented by the model profile.

The retrieval algorithm thus generates a new cloud profile from the weighted sum of structures in the cloud structure database that are consistent with the observations. The retrieval solution is:

$$\hat{\mathrm{E}}(R) = \sum_j R_j \frac{\exp\left\{-0.5\left(Tb_o - Tb_s(R_j)\right)^T (O+S)^{-1} \left(Tb_o - Tb_{s(R_j)}\right)\right\}}{\hat{\mathrm{A}}}$$

Equation 2

Where:

R_j = the vector of model profile values from the a priori database model

Tb_o = set of observed brightness temperatures

$Tb_s(x_j)$ = corresponding set of computed brightness temperatures from model profile Rj

O = observational error covariance matrices

S = model error covariance matrices

Ã, = normalization factor

The AMSR-E code searches a subset of profiles with coincident Sea Surface Temperature (SST) and Total Column Water Vapor (TCWV). TCWV is internally within the AMSR-E precipitation algorithm using an Optimal Estimation (OE) framework developed by Elsaesser and Kummerow (2008). The SST is obtained from Optimum Interpolation Sea Surface Temperatures constructed by combining observations from different platforms (satellites, ships, buoys) on a regular global grid. The satellite observations are from the AVHRR and AMSR-E instruments until 03 October 2011, and AVHRR only after that date. For more information, refer to Optimum Interpolation Sea Surface Temperature (OISST) web page. For more information on the development of the OISST, see Reynolds, et al. 2006. The same OE-based TCWV and SST climatology is also attached to the a priori database to ensure consistency between the brightness temperatures.

2.2.2.2 Instantaneous Land Rainfall

Accurate rainfall retrievals over land are far more difficult than oceanic retrievals due to the large and variable emissivity of the land surface. Specifically, the high emissivity masks the emission signature that is related directly to the water content in the atmosphere. Instead, only the brightness temperature depression due to scattering in the upper portion of clouds is observable. The scattering increases with increasing frequencies. Consequently, brightness temperature depressions at the 89-GHz channel of AMSR-E contain the least ambiguous signal of scattering by ice and/or large raindrops.

A further complication that arises over land is the lack of consistent backgrounds against which to compare the brightness temperature depression. To alleviate the problem caused by the varying emissivity associated with changes in surface characteristics such as surface wetness, snow cover, vegetation, etc. A rain/no-rain temperature depression threshold is required to screen out false identification of rain. Additionally, snow and desert surfaces cause depressed brightness temperatures at high frequencies due to surface volume scattering and can be confused with the rain signature. If these surface types are not properly screened, they can be misinterpreted as ice scattering in clouds.

GPROF 2010 Version 2 utilizes a two-step process for rain rate retrieval for the AMSR-E algorithm: rain identification and rain rate determination.

2.2.2.3 Land Rain/No Rain Determination

The rain/no rain determination results from the application of screens applied to the data retrieved at the 89-GHz channel of AMSR-E. McCollum et al. (1999) developed a methodology that adopts the GPROF approach but uses spatial information from neighboring pixels to “fill-in” indeterminate areas. See Figure 2 for a comparison between the three screening methods: NESDIS (Ferraro 1997), GSCAT2 used in the GPROF algorithm, and the new screening method.

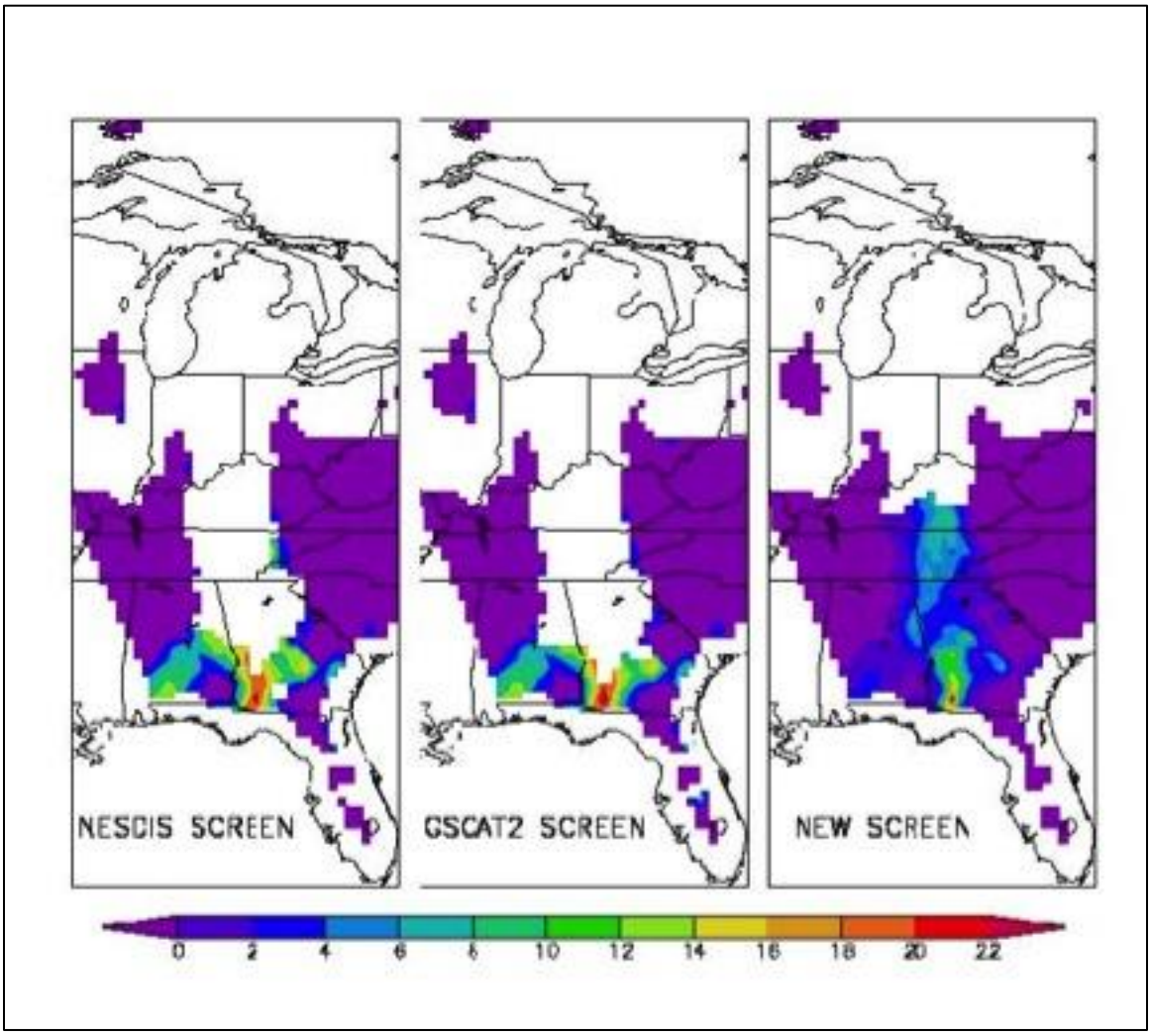

Figure 2. Comparison of Rainfall Rates (mm/h)

2.2.2.4 Land Rain Rate Determination

The AMSR-E precipitation team decided to use the same GPROF retrieval methodology as used for the ocean retrieval. Unlike the ocean component, however, the initial database of possible

profiles was carefully selected to include only those profiles that fit the empirical relation given in Equation 3.

$$RR(mm/hr)=0.00513*SIL^{1.9468}$$

Equation 3

Where:

RR = rain rate in mm/hr

SIL = Scattering Index Land

The relationship of Equation 3 was reproduced by selecting 36 profiles fitting Equation 3 from the several thousand profiles in the GPROF database (McCollum et al. 1999).

2.3 Quality, Errors, and Limitations

2.3.1 Quality Assessment

Each HDF-EOS file contains core metadata with Quality Assessment (QA) metadata flags that are set by the Science Investigator-led Processing System (SIPS) at the Global Hydrology and Climate Center (GHCC) prior to delivery to NSIDC. A separate metadata file in XML format is also delivered to NSIDC with the HDF-EOS file; it contains the same information as the core metadata. Three levels of QA are conducted with the AMSR-E Level- 2 and -3 products: automatic, operational, and science QA. If a product does not fail QA, it is ready to be used for higher-level processing, browse generation, active science QA, archive, and distribution. If a granule fails QA, SIPS does not send the granule to NSIDC until it is reprocessed. Level-3 products that fail QA are never delivered to NSIDC (Conway 2002).

2.3.2 Automatic QA

Brightness temperatures are verified to be within the physical bounds (50 K — 305 K) for all channels used by the rainfall algorithm. Automated QA for the rainfall algorithm is difficult because heavy rainfall can mask the surface, thereby hindering geo-location verification. Therefore, the rainfall algorithm relies on the Level 2A product for QA of the geo-location. As a final QA check on the computed rainfall, the brightness temperatures of the computed rainfall are compared to the observed brightness temperatures. If the difference between computed and observed brightness temperatures exceeds a pre-defined threshold, the rainfall is set to missing (pixelStatus=11).

2.3.3 Operational QA

AMSR-E Level-2A data arriving at GHCC are subject to operational QA prior to processing higher-level products. Operational QA varies by product, but it typically checks for the following criteria in a given file (Conway 2002):

- File is correctly named and sized
- File contains all expected elements
- File is in the expected format
- Required EOS fields of Time, Latitude, and Longitude are present and populated
- Structural metadata are correct and complete
- The file is not a duplicate
- The HDF-EOS version number is provided in the global attributes
- The correct number of input files were available and processed

2.3.4 Science QA

AMSR-E Level-2B data are derived from Level-2A. See AMSR-E/Aqua L2A Global Swath Spatially-Resampled Brightness Temperatures, Version 3 for further information on the QA process for the data. In the SIPS environment, the science QA includes checking the maximum and minimum variable values, and percent of missing data and out-of-bounds data per variable value. At the Science Computing Facility (SCF), also at GHCC, science QA involves reviewing the operational QA files, generating browse images, and performing the following additional automated QA procedures (Conway 2002):

- Historical data comparisons
- Detection of errors in geo-location
- Verification of calibration data
- Trends in calibration data
- Detection of large scatter among data points that should be consistent

Geo-location errors are corrected during Level-2A processing to prevent processing anomalies such as extended execution times and large percentages of out-of-bounds data in the products derived from Level-2A data.

The Team Lead SIPS (TLSIPS) developed tools for use at SIPS and SCF for inspecting the data granules. These tools generate a QA browse image in Portable Network Graphics (PNG) format and a QA summary report in text format for each data granule. Each browse file shows Level-2A and Level-2B data. These are forwarded from the Remote Sensing Systems (RSS) to the GHCC along with associated granule information, where they are converted to HDF raster images prior to delivery to NSIDC. For details, see the AMSR-E web page.

Please refer to the AMSR-E Validation Data for information about data used to check the accuracy and precision of AMSR-E observations.

2.3.5 Error Sources

Quantifying errors in this data set is complicated, because it involves understanding the nature of precipitation. Uncertainties arise when the rain layer thickness is not well understood, or when inhomogeneous rainfall occurs below the resolution of the satellite. Another potential source of error is the non-precipitating component of clouds, which contribute to brightness temperatures. Scattering-based retrievals over land also present many uncertainties, most notably the lack of a consistent relationship between frozen rain aloft and liquid at lower altitudes. Quantifying the scattering by ice is especially problematic. Ambiguities occur in the data because microwave radiation is scattered not only by rainfall and associated ice, but by snow cover and dry land (Kummerow and Ferraro 2007).

A known error exists related to sun glint that results in missing Rain Rate values, and presents as gray ovals in the AE_Rain browse images. Sun glint is not a problem over land; however, the algorithm is using only geometry to determine sun glint causing missing values to exist over land. Sun glint is included in the algorithm because it affects the brightness temperatures out to the missing radius; however, a thorough investigation is yet to be completed. Preliminary investigations indicate that the bias could be up to 15 percent in the affected areas.

2.4 Instrumentation

2.4.1 Description

Please refer to the AMSR-E Instrument Description document.

3 SOFTWARE AND TOOLS

Data are available via FTP, HTTPS, and through Reverb | ECHO, the NASA search and order tool for subsetting, reprojecting, and reformatting data. Tools that work with AMSR-E data are available on the AMSR-E Web page.

4 VERSION HISTORY

Version 3 utilizes the GPROF 2010 Version 2 algorithm and Version 3 Level-2A Brightness Temperatures as input. Version 3 now includes both rain and solid precipitation rates and types, as well as ISO lineage metadata. See the AMSR-E Data Versions Web page for a summary of algorithm changes since the start of mission.

5 CONTACTS AND ACKNOWLEDGMENTS

Dr. Christian Kummerow and Dr. David Randel
Department of Atmospheric Science
Colorado State University

Ralph Ferraro
ESSIC/CICS
2207 Computer and Space Sciences Building
University of Maryland

6 REFERENCES

Conway, D. 2002. Advanced Microwave Scanning Radiometer - EOS Quality Assurance Plan. Huntsville, AL: Global Hydrology and Climate Center.

Elsaesser, G.S., and C.D. Kummerow. 2008. Toward a fully parametric retrieval of the nonraining parameters over the global oceans. *Journal of Applied Meteorology and Climatology* 47: 1599-1618.

Ferraro, R. R. 1997. SSM/I Derived Global Rainfall Estimates for Climatological Applications. *Journal of Geophysical Research* 102: 16,715-16,735.

Ferraro, R. R., and G. F. Marks. 1995. The Development of SSM/I Rain Rate Retrieval Algorithms Using Ground Based Radar Measurements. *Journal of Atmospheric and Oceanic Technology* 12: 755-770.

Grody, N. C. 1991. Classification of Snow Cover and Precipitation Using the Special Sensor/Microwave Imager (SSM/I). *Journal of Geophysical Research* 96: 7423-7435.

Kummerow, C., R. Ferraro, and David Randell. 2014. EOS/AMSR Rainfall: Algorithm Theoretical Basis Document, Version 2 GPROF 2010 L2A. Fort Collins, Colorado, USA: Colorado State University. (PDF file, 714 KB)

Kummerow, C., Y. Hong, W. S. Olson, S. Yang, R. F. Adler, J. McCollum, R. Ferraro, G. Petty, D. B. Shin, and T. T. Wilheit. 2001. The Evolution of the Goddard Profiling Algorithm (GPROF) for Rainfall Estimation from Passive Microwave Sensors. *Journal of Applied Meteorology* 40: 1801-1820.

Kummerow, C. D., S. Ringerud, J. Crook, D. Randel and W. Berg, 2010. An observationally generated A-Priori database for microwave rainfall retrievals, *Journal of Atmospheric and Oceanic Technology* 28(2): 113-130, doi: 10.1175/2010JTECHA1468.1.

Kummerow, C., and R. Ferraro. 2006. [Supplement] EOS/AMSR-E Level-2 Rainfall: Algorithm Theoretical Basis Document. Fort Collins, Colorado, USA: Colorado State University. (PDF file, 245 KB)

Kummerow, C., and R. Ferraro. 2012. [Supplement] Algorithm Theoretical Basis Document: EOS/AMSR-E Level-2 Rainfall. Fort Collins, Colorado, USA: Colorado State University. (PDF file, 87 KB)

Kummerow, C., W. Olson, and L. Giglio. 1996. The Evolution of the Goddard Profiling Algorithm (GPROF) for Rainfall Estimation from Passive Microwave Sensors. *IEEE Transactions on Geosciences and Remote Sensing* 34: 1213-1232.

McCollum, J., and R. Ferraro. 2003. Next Generation of NOAA/NESDIS TMI, SSM/I, and AMSR-E Microwave Land Rainfall Algorithms. *Journal of Geophysical Research - Atmospheres* 108(D8): art. no. 8382.

McCollum, J. R., A. Gruber, and M. B. Ba. 1999. Discrepancy between gauges and satellite estimates of rainfall in equatorial Africa. *Journal Applied Meteorology* 41: 1065-1080.

Reynolds, R.W., T.M. Smith, C. Liu, D.B. Chelton, K.S. Casey, and M.G. Schlax, 2006: Daily high-resolution-blended analyses for sea surface temperature. *Journal of Climate* 20: 5473- 5496.

Wilheit, T., C. Kummerow, and R. Ferraro. 2003. Rainfall algorithms for AMSR-E. *IEEE Transactions on Geosciences and Remote Sensing* 41(2): 204-214.

For more information regarding related publications, see the Research Using AMSR-E Data web page.

7 DOCUMENT INFORMATION

Table 6. Acronyms and Abbreviations

Acronym	Description
AMSR-E	Advanced Microwave Scanning Radiometer - Earth Observing System
EOS	Earth Observing System
FTP	File Transfer Protocol
GHCC	Global Hydrology and Climate Center
GSFC	Goddard Space Flight Center
HDF-EOS	Hierarchical Data Format - EOS
NASA	National Aeronautics and Space Administration
NSIDC	National Snow and Ice Data Center

Acronym	Description
OISST	Optimum Interpolation Sea Surface Temperature
PNG	Portable Network Graphics
QA	Quality Assessment
RSS	Remote Sensing Systems
SCF	Science Computing Facility
SIPS	Science Investigator-led Processing System
SST	Sea Surface Temperature
TAI	International Atomic Time
TCWV	Total Column Water Vapor
TLSIPS	Team Lead SIPS
TMI	Tropical Rainfall Measuring Mission Microwave Imager
TPW	Total Precipitable Water
TRMM	Tropical Rainfall Measuring Mission
UTC	Universal Time, Coordinated

7.1 Publication Date

October 2015

7.2 Date Last Updated

07 April 2021